Bioelectrochemistry 128 (2019) 109–117

Contents lists available at ScienceDirect

Bioelectrochemistry

journal homepage: www.elsevier.com/locate/bioelechem

Effect of control mode on the sensitivity of a microbial fuel cell biosensor with *Shewanella loihica* PV-4 and the underlying bioelectrochemical mechanism

Yue Yi [a,b,c], Beizhen Xie [a,b,c], Ting Zhao [a,b,c], Ziniu Qian [a,b,c], Hong Liu [a,b,c,*]

[a] Beijing Advanced Innovation Center for Biomedical Engineering, Beihang University, Beijing 100191, China
[b] Institute of Environmental Biology and Life Support Technology, School of Biological Science and Medical Engineering, Beihang University, Beijing 100191, China
[c] International Joint Research Center of Aerospace Biotechnology & Medical Engineering, Beihang University, Beijing 100191, China

ARTICLE INFO

Article history:
Received 14 February 2019
Received in revised form 1 April 2019
Accepted 1 April 2019
Available online 2 April 2019

Keywords:
Microbial fuel cell
Biosensor
Control mode
Shewanella loihica
Biofilm viability

ABSTRACT

A relatively poor sensitivity is a critical challenge for the application of microbial fuel cell biosensors (MFC-biosensors). This study investigated the effects of two control modes on sensor sensitivity and revealed the underlying bioelectrochemical mechanism. The results demonstrated that the sensitivity of an *S. loihica* PV-4 MFC-biosensor increased by 6.1 times when the anode was controlled at a constant potential (CP) instead of being operated with a fixed external resistance (ER). This obvious difference in sensor sensitivity was partly attributed to the masking effect of the observable offset current under ER mode and the lower electricity production capacity under CP mode. Moreover, the analysis of metabolic structure showed that under CP mode the anodic biofilm presented lower viability after toxic shock, due to a poorer ability to synthesize and secrete extracellular polymeric substances. Electrochemical measurements further revealed a lower capacitance under CP mode, which favored the permeation of Cd^{2+} into the biofilm.

1. Introduction

Acute water pollution is one of the major factors threatening human security. Early warning systems for water quality monitoring can achieve timely detection of toxic agents in the aquatic environment, which is of significance for the assurance of public health. Traditional water quality monitoring is usually conducted using physicochemical methods. Though based on complex devices and complicated operation procedures, these methods enable the accurate quantification of common pollutants. However, they fail to reflect the biotoxicity of multiple contaminants and are not suitable for *insitu* and online monitoring [1]. Generic biosensors can compensate for the deficiencies of physicochemical methods and have been extensively applied for water quality monitoring. Fish, algae, invertebrates and bioluminescent bacteria are common testing organisms [2], as they can indicate the biotoxicity of a water sample based on changes in behaviors or in metabolic characteristics. Nevertheless, additional transducers which can convert biological responses to measurable electrical signals are indispensable to these biosensors. This element, however, would increase the complexity and cost of these traditional biosensors. Recently, water quality monitoring based on microbial fuel cell (MFC) technology, which uses an anodic biofilm as the sensing and transducing element, simplifies the operational process and is considered to be a novel and promising candidate for future application [3].

The MFC is a device which can utilize electricigens as catalysts to convert chemical energy from organic matter into electricity [4]. When an MFC is used as a biosensor (MFC-biosensor), the presence of toxic agents in the water sample will alter or block the extracellular electron transfer (EET) process of electricigens and further impact on MFC output. Hence, on-line monitoring of water quality can be achieved by tracking the voltage or current of an MFC-biosensor. The major advantages of the MFC-biosensor are high robustness and self-sustainability due to the anodic biofilm serving as the sensing element [5]. However, using such a biofilm as sensing element might cause deterioration of sensor sensitivity to some extent. This is because the extracellular polymeric substances (EPS), which are essential to biofilm formation, play a critical role in the protection of microbes from toxic agents [6]. Therefore, enhancing sensor sensitivity and addressing this limitation is of significance for the application of the MFC-biosensor in real world water monitoring.

A great deal of research has been conducted to optimize the configuration [7,8], shear rate [9,10], flow mode [11], external resistance [12] and cathode/anode ratio [13] of the MFC-biosensor, which can partly improve sensor sensitivity. However, the operational parameters have differed between MFC-biosensors and optimal performance might not be generalized. The control mode is another key factor affecting sensor

* Corresponding author at: School of Biological Science and Medical Engineering, Beihang University, 37 Xueyuan RD, Haidian DIST, Beijing 100191, China.
E-mail address: LH64@buaa.edu.cn (H. Liu).

https://doi.org/10.1016/j.bioelechem.2019.04.001
1567-5394/

sensitivity. In most of the previous studies, the anode and cathode of the MFC is connected to an external resistance (ER) to form a closed circuit. Under this mode, a toxic event is monitored by tracking the change in the output voltage or in the current across the ER [14,15]. Another alternative mode is to control the anode at a constant potential (CP) and measure the current generated to monitor the toxic event. Stein et al. [16] first proposed this mode and reported that the MFC-biosensor could deliver better sensitivity under CP mode. Similar results were further demostrated over a broad range of anode potentials and various corresponding resistances [11], which suggested that CP mode might be widely applicable for improving sensor sensitivity.

Although, obvious enhanced sensitivity under CP mode was observed in both studies [11,16], the bioelectrochemical mechanism for this difference has not been specified. A common phenomenon in the two studies was that when toxic shock occurred, the anode potential increased under ER mode while remaining unchanged under CP mode. It was speculated that four possible mechanisms, resulting from the increased anode potential, could possibly contribute to the different sensor sensitivities. Firstly, an offset current which could mask the inhibition of the electricity generation capacity of electricigens, might develop under ER mode. Furthermore, the substrate consumption rate of electricigens could increase with the anode potential [17], and thus the microbial activity as well as resistance to toxic agents would be affected. Additionally, the extracellular electron transfer (EET) mechanism might also change with the anode potential [18], which could result in a changed capacity for power generation. Finally, the anodic double layer capacitance behavior could vary with the anode potential [19]; this might influence the permeation of a toxic agent into the anodic biofilm. A combination of biological characterization and electrochemical analysis might contribute to clarification of possible mechanisms. Another issue in the previous studies was that the results were both based on mixed culture MFCs [11,16]. Even under identical conditions, large individual differences have been revealed between mixed culture MFCs, so this type MFC was not suitable for a study of mechanisms [4]. Moreover, the researchers of both studies investigated the responses of MFC-biosensors to only one fixed concentration of toxic shock agent, indicating a lack of quantitative comparison in sensor sensitivity between the two control modes.

To address these limitations, a pure culture (*S. loihica* PV-4) MFC-biosensor, which was considered to deliver better performance for toxicity monitoring and have a homogeneous anodic microbial community [20], was developed in this study. Toxic shocks at various concentrations of Cd^{2+} were used to quantitatively investigate the sensitivities of MFC-biosensors under different control modes. Cd^{2+} (as cadmium sulfate) was used to simulate toxic shock because of its hazardous nature and wide distribution in wastewater [21]. The main source of Cd^{2+} is industrial activity, including mining operations, nonferrous metal smelting and electroplating [22,23]. According to the British Geological Survey in 2016, the total world production of cadmium is around 26,500 tons [24]. Therefore, Cd^{2+} was normally used as a model toxic metal in previous biosensor research [3,25,26]. The underlying mechanism for the effect of control mode was further revealed by combining electrical, biochemical and biological technologies. Coulombic yield (CY) was calculated to distinguish biological electricity production and offset current, and cyclic voltammetry (CV) was employed to investigate the electron transfer process. The compositions of extracellular polymeric substances (EPS) were analyzed to explain the difference in biofilm viability. Electroactive measurements combined with theoretical analysis were conducted to interpret the changes in anodic double layer capacitance.

2. Material and methods

2.1. MFC construction

12 MFCs (MFCs 1–12) with the same H-type configuration were constructed in this study. MFCs 1–4 were used to compare the sensitivity of MFC-biosensors under different control modes, while MFCs 5–8 and MFCs 9–12 were set to investigate biological and electrochemical mechanisms, respectively. Cylindrical reagent bottles (50 mL each) sealed with polytetrafluoroethylene lids were used as the anodic and cathodic chambers, and connected *via* a glass tube (15 mm diameter, 40 mm height). A pre-treated proton exchange membrane (Nafion117, DuPont, USA) [27] was used to divide the two chambers. The anode was a 2.5 cm × 2.5 cm piece of carbon cloth (HCP330, Hesen, China), which was pre-treated with acetone and ammonia before use [28]. The cathode comprised two 2.0 cm × 2.0 cm pieces of $0.5 mg cm^{-2}$ Pt-loaded carbon paper (HCP120, Hesen, China). Two additional electrodes, including a 1 cm × 1 cm piece of Pt (Pt210, Aida, China) as the counter electrode and an Ag/AgCl electrode (R0303, AiDa, China; 0.205 V *vs* standard hydrogen electrode) as the reference electrode, were inserted into the anodic chamber through the lid for electrochemical measurement. Except for the Ag/AgCl electrode, all the parts included in the MFC were autoclaved. The Ag/AgCl electrode was soaked overnight in 75% alcohol and then sterilized with ultraviolet radiation. All the MFCs were fabricated in a laminar flow cabinet (SW-CJ-1F, Airtech, China).

2.2. MFC start up

S. loihica PV-4 (ATCC®BAA1088™, ATCC, USA) was activated overnight twice in Luria–Bertani medium after being taken out from a −80 °C fridge. Subsequently, the culture was centrifuged to remove supernatant and was resuspended in anolyte [29]. Finally, the bacterial suspension was used to inoculate MFCs 1–12 with the same inoculation ratios (30% v/v). Each liter of anolyte consisted of 2.50 g $NaHCO_3$, 0.08 g $CaCl_2 \cdot 2H_2O$, 1.00 g NH_4Cl, 0.20 g $MgCl_2 \cdot 6H_2O$, 10.00 g NaCl and 7.20 g 4-(2-hydroxyethyl)-1-piperazineethanesulfonic acid (HEPES). The catholyte only contained NaCl and HEPES at the same concentrations. Sodium lactate was added to the anolyte as carbon source with a final concentration of 10 mM [30]. After inoculation, all the MFCs were operated in ER mode during the startup process. Each anode was connected to a cathode *via* a fixed external resistance of 680 Ω and all the MFCs were operated in batch-mode at 25 °C. When the output voltage of the MFCs decreased to 50 mV, the anolyte and catholyte were both replaced in a sterile environment. During the startup process, the anolyte was forced to flow through the anode electrode and recirculated at a flow rate of 3 mL min^{-1}.

2.3. Biosensor test

After the enrichment of the biofilms, MFCs 1–4 were operated in continuous-flow mode with the same flow rate as before and anolyte containing a lower concentration carbon source (1 mM sodium lactate). Once stably operated, the four MFC-biosensors were challenged with toxic shock at specific concentration under different control modes (ER and CP). A schematic diagram of the two control modes is shown in Fig. S1. Duplicate MFC-biosensors were conducted for each control mode and all tests were performed in triplicate to guarantee repeatability. Each toxic test included three steps. Firstly, non-toxic anolyte was continuously pumped into the anodic chambers until the output voltages and anode potentials became stable. Then two MFC-biosensors (MFCs 1–2) were switched to operate in CP mode while the other two MFC-biosensors continued to be operated under ER mode. In the context of CP mode, the anode and cathode was connected to the respective working electrode and counter electrode of a potentiostat (CHI1030C, ChenHua, China), and the anode potential was kept constant as with the ER mode. Finally, when the four MFC-biosensors were re-stabilized for one hour, the influent was switched to the toxic anolyte containing specific concentration of Cd^{2+} (0.25, 0.5, or 0.75 $mg L^{-1}$) with an exposure time of 30 min. After the toxicity test, MFCs 1–2 were again switched to ER mode to obtain a faster recovery [16]. The anodic chambers of the four MFC-biosensors were drained in a sterile

environment and comprehensively fed with non-toxic anolyte. Before next test, the output voltage and internal resistance of each MFC-biosensor were measured to ensure its complete recovery.

2.4. Biofilm analysis

Similar to MFCs 1–4, four other MFC-biosensors (MFCs 5–8) were fed with a continuous flow of influent after the start-up process. After stable operation, the four MFC-biosensors were challenged with the same toxic shock (0.5 mgL^{-1} Cd^{2+}) under different control modes to compare the changes in biofilm properties. This test was performed in triplicate and was conducted in following steps. Firstly, non-toxic anolyte was continuously pumped into the anodic chambers. After the stabilization of MFC-biosensor output, a 0.5 cm × 2.5 cm piece of biofilm sample was collected from the same location at each anode. Then two MFC-biosensors (MFCs 5–6) were exposed to 0.5 mgL^{-1} Cd^{2+} for 30 min under CP mode and the others under ER mode. After the toxic event, all the MFC-biosensors were sampled again with the same sampling procedure stated above. Each biofilm sample was divided into two parts. A small part (0.5 cm × 0.5 cm piece) was used to observe the metabolic structure of the anodic biofilm, and the other part was used for EPS analysis.

The biofilm metabolic structure was observed with a confocal laser scanning microscope (CLSM, TCS SP8, Leica, Germany). Before observation, all the samples were stained for 15 min with the LIVE/DEAD® BacLight™ Bacterial Viability Kit (7012, Invitrogen, USA) and were rinsed three times with 0.85% NaCl solution. The specific excitation/emission wavelengths for the two dyes (SYTO9 and propidium iodide) used in this study were 488/500 nm and 488/635 nm, respectively. For each sample, at least three locations were randomly selected for observation and the three-dimensional structure of the biofilm was reconstructed by scanning in the z-stack mode.

The EPS of the anodic biofilms was extracted with a modified heat extraction method [31]. Before heating, the biofilm was collected from each anodic sample by vortex oscillation at 1000 rpm for 15 min. The collection was filtrated at a 0.22 μm polyethersulfone membrane and the filtrate was concentrated for EPS measurement. Protein components were measured by the Bradford method [32], while the polysaccharide components were determined by the anthrone-sulfate method [33].

2.5. Electrochemical analysis

The last four MFC-biosensors (MFCs 9–12) were used to conduct electrochemical impedance spectroscopy (EIS) at different potentials after start-up. Subsequently, the four MFC-biosensors were challenged with 0.5 mgL^{-1} Cd^{2+} for 30 min under different control modes (MFCs 9–10 under CP mode, MFCs 11–12 under ER mode). Meanwhile, CV curves were recorded before and after the toxic event to study the changes in the EET process and electrochemical activity under each control mode. After complete recovery, all four MFC-biosensors were challenged with the same toxic shock again under CP mode. Short-term amperometric (j-V) tests were conducted before and after the toxic shock according to a previous protocol [11].

All the electrochemical experiments were performed in a three-electrode system. EIS was measured *via* an electrochemical workstation (Zennium E, Zahner, Germany) with a frequency range of 10 mHz −100 kHz and a signal amplitude of 10 mV. The anode potential was controlled at 20−80 mV against the reference electrode and the settling time before the EIS measurements was 15 min. For the CV test, CV curves were recorded *via* the potentiostat at a scan rate of 10 mVs^{-1}. The scan range was −0.8−0.6 V and the holding time was 10 s. A short term j-V test was also conducted *via* the potentiostat. The initial anode potential was 20 mV and then the applied potential increased from 20 mV to 80 mV with an interval of 20 mV. Each potential was applied for 15 min and the average current in the final 15 s was defined as the stable current in each phase.

2.6. Analysis and calculations

The output voltage of the MFC was recorded by a data acquisition system (USB-1608FS, Measurement Computing Corporation, USA) with a sampling interval of 5 s. The corresponding current was calculated according to Ohm's law. CY was calculated by integrating the current over the test time. EIS data were analyzed *via* Zman 2.0 software (WonATech, South Korea) with an equivalent circuit model $R_a/Q_a + R_s$ [19]. In this model, R_s and R_a referred to the ohmic and charge transfer resistances of anode, respectively, and Q_a was a constant phase angle element [19,34]. The inhibition ratio (IR) of the current was employed to assess sensor sensitivity and can be calculated based on:

$$\mathrm{IR} = {}^{(I_n - I_t)}\Big/_{I_n} * 100\% \quad (1)$$

where I_n and I_t referred to the currents before and after toxic event, respectively [35]. The viability of the biofilm (VB) was defined as the proportion of viable bacteria in total biomass and was calculated according to:

$$\mathrm{VB} = {}^{I_v}\Big/_{(I_v + I_d)} * 100\% \quad (2)$$

where I_v and I_d were the integrated optical densities of viable and dead bacteria [36] obtained from CLSM images by Image J 1.8.0_112 software (National Institutes of Health, USA), respectively. All the potentials given in the subsequent discussion are provided with respect to an Ag/AgCl electrode reference.

3. Results and discussion

3.1. Effect of control mode on sensor sensitivity

During stable operation, the anode potentials of the MFC-biosensors stabilized at approximately 50 mV and thus under CP mode the anode potentials were constantly controlled at this value during the detection of Cd^{2+}. The performance of the MFC-biosensors (MFCs 1–4) challenged with 0.5 mgL^{-1} Cd^{2+} shock under the two control modes (CP and ER) is shown in Fig. 1a. It could be seen that the MFC-biosensors generated stable currents with a fluctuation of less than 5% before the toxic event. When the influent was switched to toxic anolyte (in the 600th second), under CP mode the current decreased dramatically and reached a new steady state after 15 min of exposure, resulting in a final IR of 27.4% after 30 min of exposure. By contrast, the response of the MFC-biosensor under ER mode was quite different (Fig. 1b). Although a decrease in current was also observed after the toxic shock, the rate of decline was much slower than that under CP mode, suggesting a mild inhibition of microbial activity under ER mode. After 30 min toxic exposure IR merely achieved 5.5%, indicating a low sensitivity to the toxic shock under ER mode. Moreover, the anode potential increased from 48.0 mV to 59.3 mV as the toxic event occurred and still presented an uptrend at the end of the event (Fig. 1b).

The higher sensitivity of the MFC-biosensor under CP mode was further verified by conducting Cd^{2+} shocks at various concentrations. As shown in Fig. 1c, the IR at each concentration was much higher under CP mode. Meanwhile, IR under the two control modes increased with the concentration of Cd^{2+} and two good linear relationships were observed ($R^2 = 0.99$ for CP mode, $R^2 = 0.93$ for ER mode). The sensitivity of the MFC-biosensor can be quantified by the slope of the IR-concentration relationship [7]. In this study, the sensitivity for the detection of Cd^{2+} was 65.1%/ppm under CP mode while only 9.2%/ppm under ER mode. This result indicates that the sensor sensitivity can be enhanced 6.1 times when the MFC-biosensor was operated with CP mode.

The four MFC-biosensors shared the same configuration and culture conditions. Therefore, the discrepancies in sensor sensitivity could be

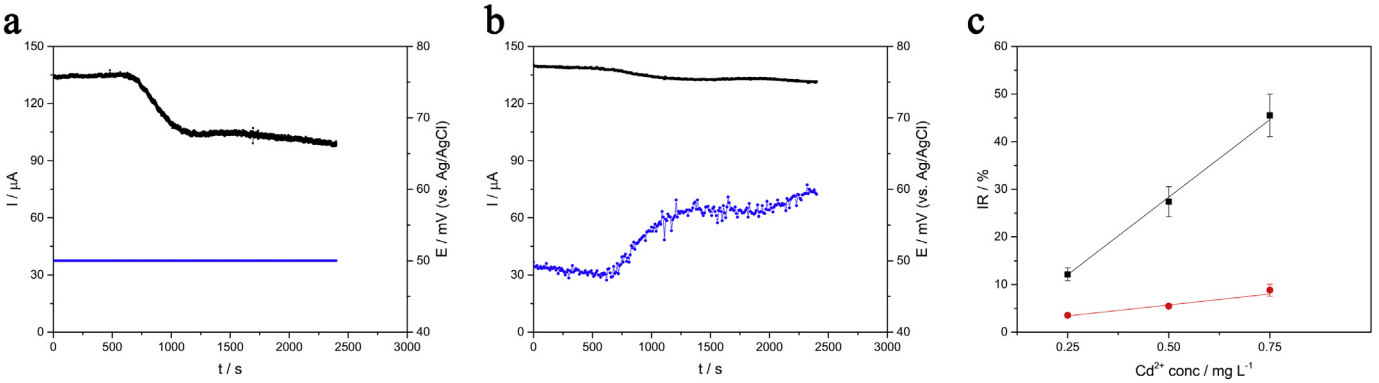

Fig. 1. (a) Output current (black line) and anode potential (blue line) of an MFC-biosensor challenged with 0.5 mgL^{-1} Cd^{2+} shock under CP mode. (b) Output current (black line) and anode potential (blue line) of an MFC-biosensor challenged with 0.5 mgL^{-1} Cd^{2+} shock under ER mode. (c) Relationships and fitting lines between Cd^{2+} concentrations and IR under CP (black square) and ER (red circle) modes.

attributed to the different control modes. Notably, the anode potentials were about 50 mV under non-toxic condition with both control modes. During a toxic event, the anode potential increased continuously under ER mode and remained constant under CP mode due to potentiostatic control (Fig. 1a-b). The increased anode potential will release negative charge into the circuit and thus cause an offset current, which has the same direction as the current generated by the electricigens. Thereby, the inhibition of electricity generation induced by a toxic shock might be masked. Furthermore, the electrochemical activity of a biofilm could also vary with the anode potential. In order to investigate the effect of the control mode on the anodic reaction, the CYs generated under non-toxic condition as well as during the toxic shock were calculated, shown in Fig. 2. As the initial anode potentials were almost the same, the electricity production capacities under non-toxic conditions were similar under the two modes (232.0 mC/2400 s and 240.3 mC/2400 s for CP and ER modes, respectively). When the MFC-biosensor was exposed to 0.5 mgL^{-1} Cd^{2+} shock, an obvious difference in CY was observed (171.1 mC/2400 s for CP mode, 232.0 mC/2400 s for ER mode). Different from CP mode, the CY under ER mode derived from the offset current and the bioelectrochemical reaction at the anode. Based on charge conservation, the CY from the latter source can be calculated and it was 199.6 mC/2400 s under ER mode, while still <171.1 mC/2400 s under CP mode. This phenomenon indicates that the same toxic shock results in a poorer electricity generation capacity of electricigens under CP mode.

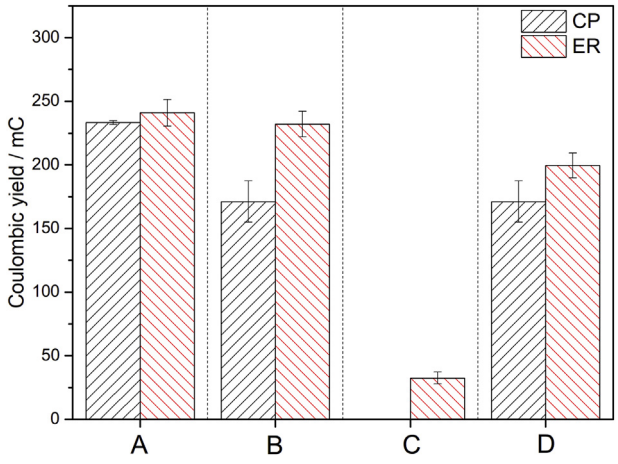

Fig. 2. Electricity generation capacities under the two control modes. Total CYs under non-toxic condition (A) and toxic condition (B). The CYs due to the increase of anode potential (C) and bioelectrochemical reaction in anode (D).

3.2. Effect of control mode on extracellular electron transfer mechanism and microbial activity

The increased anode potential might impact microbial electricity generation capacity in two ways. *Shewanella* can employ different EET processes at different potentials [18], hence the changed potential might alter the electron transfer pathway and further affect electricity generation capacity. Meanwhile, potential can significantly affect the activity of anodic biofilm [37], also resulting in different electricity production capacities at different potentials.

CV is widely used to study the electron transfer mechanisms and bioelectrocatalytic activity of electrode biofilms [38]. As shown in Fig. 3, CV curves were measured under the two modes before and after a 0.5 mgL^{-1} Cd^{2+} toxic event. All the curves showed a typical sigmoid shape, which was consistent with the Nernst-Monod equation [39]. Under non-toxic condition, a major redox system was observed (Fig. 3a-b), with an oxidation peak at −0.066 V and a reduction peak at −0.254 V, respectively. This pair of peaks centered at approximate −0.160 V, which was probably related to outermembrane c-type cytochromes that control the direct electron transfer (DET) process [40]. Another electron transfer pathway, *i.e.*, electron transfer through a mediator (MET), has also been found in *Shewanella* [41]. In the MET process, electron transfer is completed through an additional or a self-secreted mediator (*e.g.*, riboflavin), which commonly shows a more negative peak potential in CV curves according to a previous study [37]. However, MET was not observed in this study, which might be due to the fact that *S. loihica* tends to generate electricity *via* the DET process in the context of a high anode potential (50 mV). Meanwhile, the continuous flow in anodic chamber is not favorable to the accumulation of redox mediator [42].

As shown in Fig. 3a-b, the CV curves recorded after the toxic shock appeared as a similar sigmoid shape and the peak potentials remained constant as before. Moreover, no additional redox system emerged after the toxic event under the two modes; this phenomenon suggests that the electron transfer pathway do not change during the detection of Cd^{2+} under both modes. However, an apparent decline in limiting current density could be observed after the toxic shock and an obvious difference was noted between the two modes. The current density decreased from 4.1Am^{-2} to 3.3Am^{-2} under CP mode while it only dropped by 0.1 Am^{-2} (from 3.9 Am^{-2} to 3.8 Am^{-2}) under ER mode. The descent rate (DR) of the limiting current density is defined as the portion of the decrease of the limiting current density after the toxic shock, which can reflect the redox property changes of biofilms induced by toxic agents [36]. In this study, DR was 16.3% under CP mode while only 4.7% under ER mode (Fig. 3c), indicating more severe damage to bioelectrochemical activity after the same toxic event under CP mode.

The more serious damage of biofilm activity under the CP mode could be demonstrated by the CLSM images more directly (Fig. 4a-d).

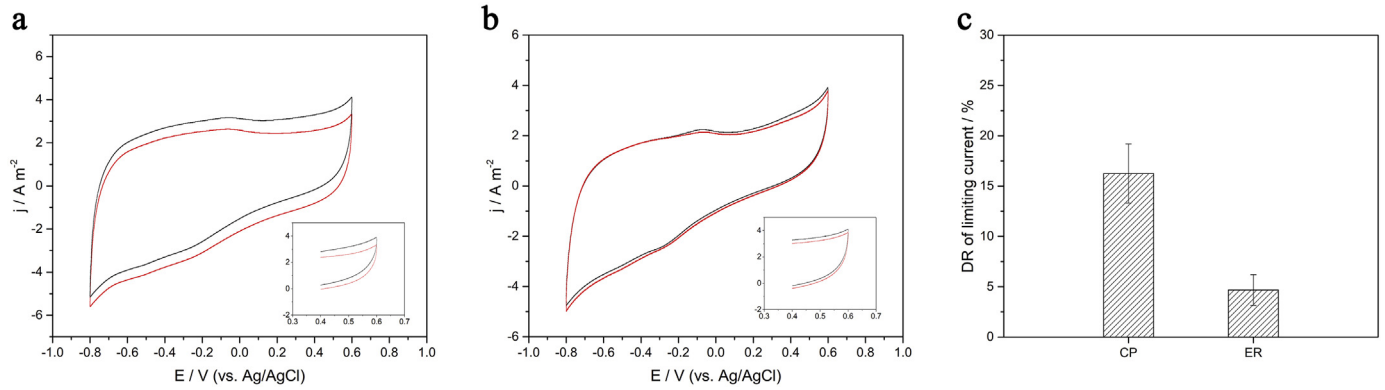

Fig. 3. (a) CV curves before (black line) and after (red line) the toxic shock under CP mode. (b) CV curves before (black line) and after (red line) the toxic shock under ER mode. (c) The DR of limiting current densities under the two modes.

Based on the differences in the permeability of cell membrane, viable bacteria were imaged as green while dead bacteria as red. It is clearly shown that the anode surface was almost entirely colonized with alive bacteria before the toxic shock (Fig. 4a, c), suggesting a high biofilm viability under non-toxic condition. Calculated from integrated optical densities [36,43], the viable bacteria proportions under the two modes were 95.6% (CP mode) and 97.7% (ER mode), respectively. After the exposure to 0.5 mgL^{-1} Cd^{2+} for 30 min, dead bacteria increased obviously (Fig. 4b, d) under the two control modes; this was due to that the presence of Cd^{2+} could change the functional groups on cell walls and inactivate the intracellular enzymes [44]. However, the proportion of viable bacteria presented a larger decline under CP mode. It sharply decreased from 95.6% to 48.3% while it only dropped to 79.7% under ER mode. This result suggests that the anodic biofilms with similar activity present quite different resistance to toxic agents under different control modes.

3.3. Bioelectrochemical mechanism for the effect of control mode on sensor sensitivity

EPS plays an important role in the self-protection of a biofilm and functions as a protective barrier to hinder the intracellular penetration of heavy metals. Therefore, it is regarded as one of the indicators of microbial resistance to toxic agents [45]. In this study, the EPS contents clearly increased under the two control modes after the toxic shock (Fig. 5a), indicating that exposure to Cd^{2+} could activate the self-protection mechanism and promote the secretion of EPS [46]. However, the enhanced EPS contents showed an apparent difference under the two control modes (28.2 μg cm^{-2} under ER mode and 11.4 μgcm^{-2} under CP mode), suggesting that the anodic biofilm under ER mode possessed a higher resistance to toxic agents.

The protein (PN) components in EPS, which contain some negatively charged functional groups (*e.g.*, carboxyl and hydroxyl) and might effectively bind metal cations, are a key factor for a biofilm to attenuate the toxicity of a heavy metal [47]. In this study, the secretion of PN was greatly stimulated due to Cd^{2+} shock under both modes (Fig. 5b). Notably, it increased by 155.3% under ER mode (from 15.4 μgcm^{-2} to 38.8 μgcm^{-2}) while only 64.1% under the CP mode (14.5 μgcm^{-2} to 23.8 μgcm^{-2}). Meanwhile, the changes in the polysaccharide (PS) content of EPS followed a similar trend (Fig. 5c); it increased by 57.8% and 26.3% under ER and CP modes, respectively. This phenomenon suggests that the anodic biofilm under CP mode has a lower resistance to a toxic agent due to the poorer ability to synthesize and secrete EPS, and thus the MFC-biosensor under CP mode delivered higher sensitivity than ER mode.

The synthesis and secretion of EPS requires a large amount of energy [48], which derives from the oxidation reaction at anode [49]. The current generation of the MFC is considered to be an indicator of the reaction rate and can be calculated according to the previous studies [50,51] by:

$$i = {(\varphi_{eq} - \varphi_a)} \Big/ {R_a} \tag{3}$$

where i is the current generated, φ_{eq} is the initial anode potential (*i.e.*, the equilibrium potential), φ_a is the actual anode potential and R_a is the charge transfer resistance of anode. A previous study has demonstrated that φ_a had an obvious effect on R_a [19], which can be assessed by EIS measurement at different anode potentials. As shown in Fig. 6a, the diameter of the semicircle in the Nyquist impedance spectra largely increased as anode potential decreased. According to the fitted results, R_a was only 34.4 Ω at 80 mV, which sharply dropped from the 283.2 Ω at 20 mV (Fig. 6b). This phenomenon suggests that the rising anode potential can increase the overpotential (φ_a–φ_{eq}) and decrease R_a simultaneously, resulting in a higher magnitude of current and electroactivity of the biofilm. Thereby, the increased anode potential might be favorable for the synthesis and secretion of EPS under ER mode. Moreover, due to the fact that electron transfer rate is usually higher than the electrode reaction rate, positive charge commonly accumulates on the electrode surface with anodic polarization [52]. The magnitude of residual charge (q) can be obtained according to:

$$q = \int_{\varphi_0}^{\varphi_a} C d\varphi, \tag{4}$$

where C is the double-layer capacitance and φ_0 is the zero-charge potential. The anode non-ideal capacitance (C_a) can be calculated based on the fitting results of R_a and Q_a [53]. As shown in Fig. 6c, C_a increased from 22.8 mF at 20 mV to 25.7mF at 80 mV, presenting a similar trend as a previous study [19]. This phenomenon indicates that q will increase with φ_a. Therefore, the increased anode potential under ER mode might be detrimental to the permeation of homocharge Cd^{2+} into the biofilm. This might be the reason why the anode potential still presented an upward trend after the MFC-biosensor was exposed to Cd^{2+} for 30 min under this mode (Fig. 1b).

To further verify the conjecture above and optimize anode potential under CP mode, four MFC-biosensors were challenged with toxic shock under CP mode and short term j-V curves were recorded before and after the shock. The corresponding IR values at different potentials were calculated and are presented in Fig. 6d. Notably, IR reached 30.7% at 20 mV while decreased to 25.0% at 80 mV. This result suggests that the increase in anode potential will diminish the response of MFC-biosensor and a lower anode potential should be set to enhance its sensitivity under CP mode.

In this study, one toxic pollutant (*i.e.* Cd^{2+}) was chosen to quantify the effect of control modes on MFC-biosensor sensitivity. However,

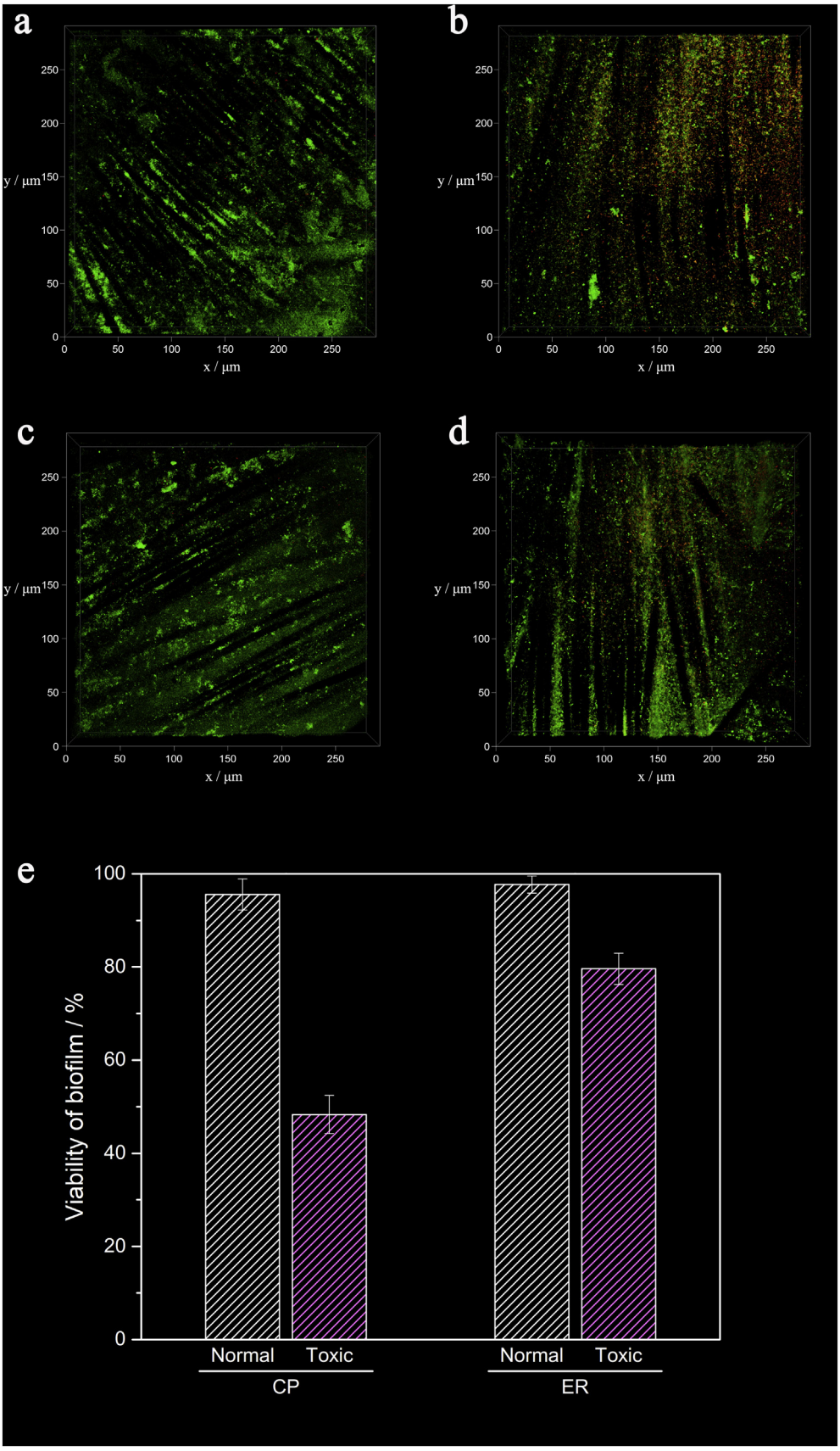

Fig. 4. Metabolic structures and viabilities of anodic biofilms. The metabolic structures before (a) and after (b) the toxic shock under CP mode. The metabolic structures before (c) and after (d) the toxic shock under ER mode. The viabilities of biofilms (e).

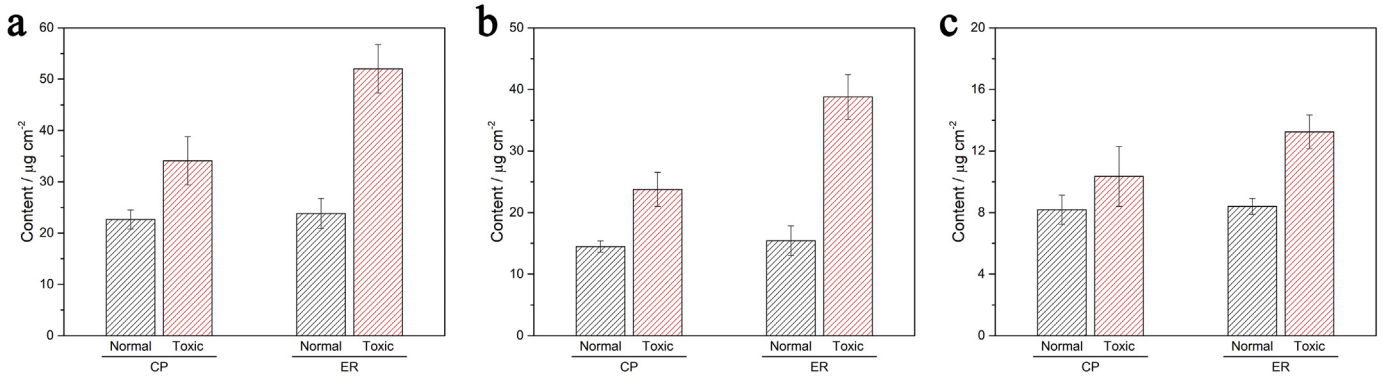

Fig. 5. EPS contents (a), PN contents (b) and PS contents (c) before and after toxic shock under the two control modes.

water pollution emergencies usually occur as combined contamination in real aquatic environment [12]. Different types of toxic pollutants (*e.g.* heavy metals, organic contaminants, acidic and basic components) may coexist in the polluted water. Due to the known biotoxicity of these substances, it is reasonable to infer that an MFC-biosensor operated with CP mode can provide more sensitive warning when these substances present. However, the enhanced sensitivity of an MFC-biosensor with CP mode might also increase the false warning caused by the changes of the water conductivity or the organic matter. Previous studies have proposed some measures to reduce the false signal of the MFC-biosensor, such as adding high concentration NaCl to the water sample to avoid the effect of conductivity on the MFC-biosensor [54] and optimizing the background concentration of organic matter in water [55]. Nevertheless, a systematic optimization research on the accuracy of toxicity assessment by an MFC-biosensor under CP mode has not been reported yet and needs further study in the future.

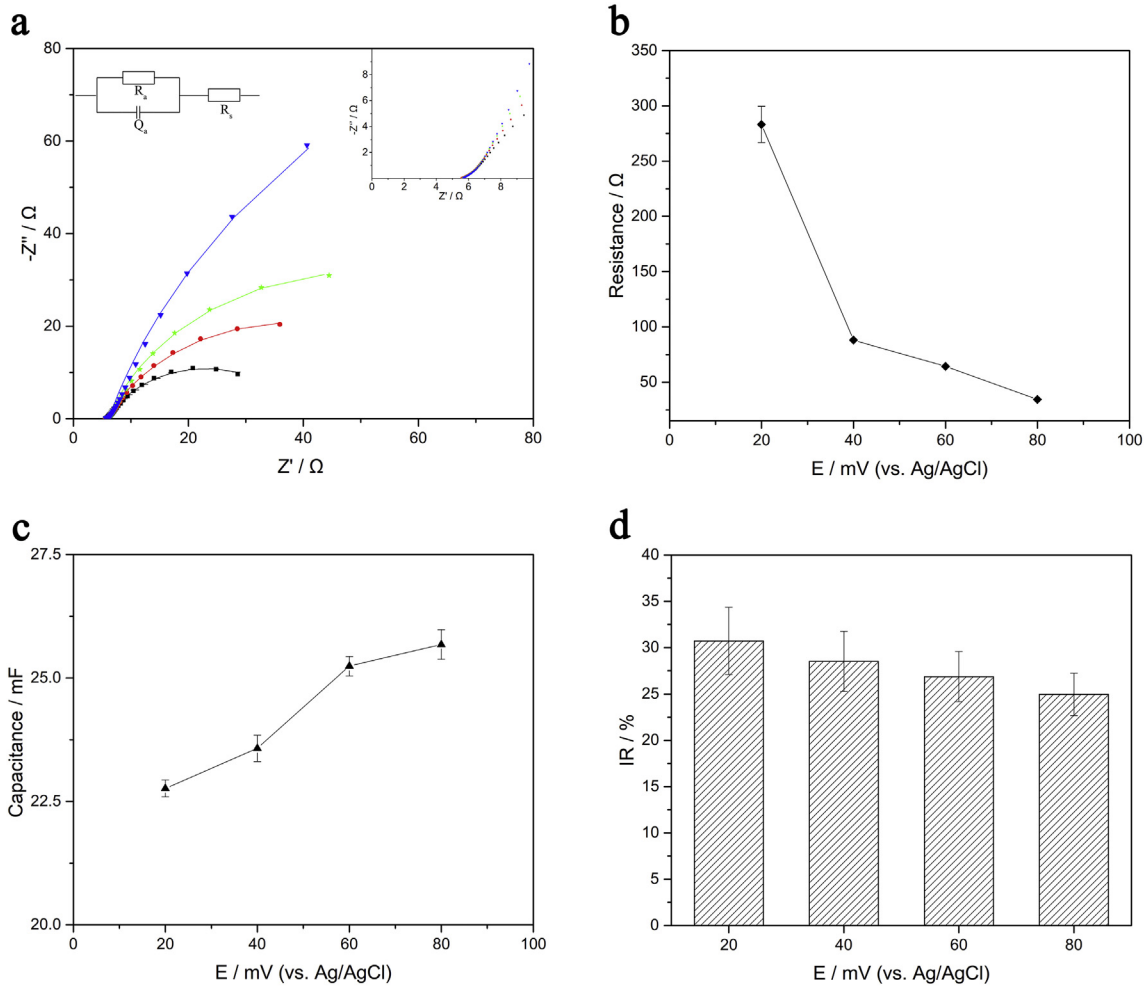

Fig. 6. Effect of the anode potential on biofilm electroactivity and sensor sensitivity. (a) The Nyquist plots at different anode potentials: 20 mV (blue triangle), 40 mV (green star), 60 mV (red circle) and 80 mV (black square). (b) The values of the anode charge transfer resistance R_a at different potentials. (c) The values of the anode non-ideal capacitance C_a at different potentials. (d) The IR values at different potentials.

4. Conclusions

The sensitivity of the *S. loihica* PV-4 MFC-biosensor increased by 6.1 times when it was operated in CP mode instead of ER mode. The biological analysis coupling with the electrochemical measurement revealed the underlying mechanism. The increased anode potential after toxic shock under ER mode resulted in the generation of offset current and higher resistance to toxic agents, which largely deteriorated the sensor sensitivity. For detecting positive charged pollutants, a low potential setting was more applicable to obtaining higher sensitivity. Future study will optimize anode potentials for detecting different types of pollutants.

Supplementary data to this article can be found online at https://doi.org/10.1016/j.bioelechem.2019.04.001.

Acknowledgements

This work was financially supported by grants from the National Natural Science Foundation of China [31770135]; Beijing Municipal Science & Technology Commission [Z171100000717013]; National Undergraduate's Innovation and Entrepreneurship Training Program [201610006085]; and the Fundamental Research Funds for the Central Universities.

References

[1] M.H. Banna, S. Imran, A. Francisque, H. Najjaran, R. Sadiq, M. Rodriguez, M. Hoorfar, Online drinking water quality monitoring: review on available and emerging technologies, Crit. Rev. Environ. Sci. Technol. 44 (2014) 1370–1421.
[2] S.H.A. Hassan, S.W. Van Ginkel, M.A.M. Hussein, R. Abskharon, S.E. Oh, Toxicity assessment using different bioassays and microbial biosensors, Environ. Int. 92–93 (2016) 106–118.
[3] M. Kim, M.S. Hyun, G.M. Gadd, H.J. Kim, A novel biomonitoring system using microbial fuel cells, J. Environ. Monit. 9 (2007) 1323–1328.
[4] B.E. Logan, J.M. Regan, Electricity-producing bacterial communities in microbial fuel cells, Trends Microbiol. 14 (2006) 512–518.
[5] Y. Jiang, X.F. Yang, P. Liang, P.P. Liu, X. Huang, Microbial fuel cell sensors for water quality early warning systems: fundamentals, signal resolution, optimization and future challenges, Renew. Sust. Energ. Rev. 81 (2018) 292–305.
[6] T.T. More, J.S.S. Yadav, S. Yan, R.D. Tyagi, R.Y. Surampalli, Extracellular polymeric substances of bacteria and their potential environmental applications, J. Environ. Manag. 144 (2014) 1–25.
[7] M. Di Lorenzo, A.R. Thomson, K. Schneider, P.J. Cameron, I. Ieropoulos, A small-scale air-cathode microbial fuel cell for on-line monitoring of water quality, Biosens. Bioelectron. 62 (2014) 182–188.
[8] Y. Jiang, P. Liang, P.P. Liu, X.X. Yan, Y.H. Bian, X. Huang, A cathode-shared microbial fuel cell sensor array for water alert system, Int. J. Hydrog. Energy 42 (2017) 4342–4348.
[9] A. Fraiwan, S. Sundermier, D. Han, A.J. Steckl, D.J. Hassett, S. Choi, Enhanced performance of micro-electro-mechanical-systems (MEMS) microbial fuel cells using electrospun microfibrous anode and optimizing operation, Fuel Cells 13 (2013) 336–341.
[10] Y.J. Shen, M. Wang, I.S. Chang, H.Y. Ng, Effect of shear rate on the response of microbial fuel cell toxicity sensor to Cu (II), Bioresour. Technol. 136 (2013) 707–710.
[11] Y. Jiang, P. Liang, C.Y. Zhang, Y.H. Bian, X.F. Yang, X. Huang, P.R. Girguis, Enhancing the response of microbial fuel cell based toxicity sensors to Cu (II) with the applying of flow-through electrodes and controlled anode potentials, Bioresour. Technol. 190 (2015) 367–372.
[12] Y. Yi, B.Z. Xie, T. Zhao, Z.M. Li, D. Stom, H. Liu, Effect of external resistance on the sensitivity of microbial fuel cell biosensor for detection of different types of pollutants, Bioelectrochemistry 125 (2019) 71–78.
[13] N. Uría, D. Sánchez, R. Mas, O. Sánchez, F.X. Munoz, J. Mas, Effect of the cathode/anode ratio and the choice of cathode catalyst on the performance of microbial fuel cell transducers for the determination of microbial activity, Sens. Actuators B-Chem. 170 (2012) 88–94.
[14] C.J. Feng, A.Y. Hu, S.H. Chen, C.P. Yu, A decentralized wastewater treatment system using microbial fuel cell techniques and its response to a copper shock load, Bioresour. Technol. 143 (2013) 76–82.
[15] D.B. Yu, L. Bai, J.F. Zhai, Y.Z. Wang, S.J. Dong, Toxicity detection in water containing heavy metal ions with a self-powered microbial fuel cell-based biosensor, Talanta 168 (2017) 210–216.
[16] N.E. Stein, H.V.M. Hamelers, C.N.J. Buisman, The effect of different control mechanisms on the sensitivity and recovery time of a microbial fuel cell based biosensor, Sens. Actuators B-Chem. 171 (2012) 816–821.
[17] X. Wang, Y.J. Feng, N.Q. Ren, H.M. Wang, H. Lee, N. Li, Q.L. Zhao, Accelerated start-up of two-chambered microbial fuel cells: effect of anodic positive poised potential, Electrochim. Acta 54 (2009) 1109–1114.
[18] H.A. Liu, S. Matsuda, S. Kato, K. Hashimoto, S. Nakanishi, Redox-responsive switching in bacterial respiratory pathways involving extracellular electron transfer, Chemsuschem 3 (2010) 1253–1256.
[19] X.P. Zhu, J.C. Tokash, Y.Y. Hong, B.E. Logan, Controlling the occurrence of power overshoot by adapting microbial fuel cells to high anode potentials, Bioelectrochemistry 90 (2013) 30–35.
[20] Y. Yi, B.Z. Xie, T. Zhao, H. Liu, Comparative analysis of microbial fuel cell based biosensors developed with a mixed culture and *Shewanella loihica* PV-4 and underlying biological mechanism, Bioresour. Technol. 265 (2018) 415–421.
[21] S. Chowdhury, M.A.J. Mazumder, O. Al-Attas, T. Husain, Heavy metals in drinking water: occurrences, implications, and future needs in developing countries, Sci. Total Environ. 569 (2016) 476–488.
[22] C.P.C. Poon, Removal of cadmium from wastewaters, Experientia 40 (1984) 127–136.
[23] K. Pyrzynska, Removal of cadmium from wastewaters with low-cost adsorbents, J. Environ. Chem. Eng. 7 (2018) 102795.
[24] T.J. Brown, N.E. Idoine, E.R. Raycraft, R.A. Shaw, S.F. Hobbs, P. Everett, E.A. Deady, T. Bide, World Mineral Production 2012–16, British Geological Survey, 2018.
[25] S. Kumar, N. Verma, A.K. Singh, Development of cadmium specific recombinant biosensor and its application in milk samples, Sensors Actuators B Chem. 240 (2017) 248–254.
[26] A. Ivask, T. Rõlova, A. Kahru, A suite of recombinant luminescent bacterial strains for the quantification of bioavailable heavy metals and toxicity testing, BMC Biotechnol. 9 (2009) 41.
[27] M. Ghasemi, W.R.W. Daud, M. Ismail, M. Rahimnejad, A.F. Ismail, J.X. Leong, M. Miskan, K. Ben Liew, Effect of pre-treatment and biofouling of proton exchange membrane on microbial fuel cell performance, Int. J. Hydrog. Energy 38 (2013) 5480–5484.
[28] S.A. Cheng, B.E. Logan, Ammonia treatment of carbon cloth anodes to enhance power generation of microbial fuel cells, Electrochem. Commun. 9 (2007) 492–496.
[29] T. Liu, Y.Y. Yu, D.Z. Li, H. Song, X.L. Yan, W.N. Chen, The effect of external resistance on biofilm formation and internal resistance in *Shewanella* inoculated microbial fuel cells, RSC Adv. 6 (2016) 20317–20323.
[30] D. Wu, D.F. Xing, L. Lu, M. Wei, B.F. Liu, N.Q. Ren, Ferric iron enhances electricity generation by *Shewanella oneidensis* MR-1 in MFCs, Bioresour. Technol. 135 (2013) 630–634.
[31] S.W. Li, G.P. Sheng, Y.Y. Cheng, H.Q. Yu, Redox properties of extracellular polymeric substances (EPS) from electroactive bacteria, Sci. Rep. 6 (2016) 39098.
[32] M.M. Bradford, A rapid and sensitive method for the quantitation of microgram quantities of protein utilizing the principle of protein-dye binding, Anal. Biochem. 72 (1976) 248–254.
[33] J.H. Roe, The determination of sugar in blood and spinal fluid with anthrone reagent, J. Biol. Chem. 212 (1955) 335–343.
[34] N. Garino, A. Sacco, M. Castellino, J.A. Muñoz-Tabares, M. Armandi, A. Chiodoni, C.F. Pirri, One-pot microwave-assisted synthesis of reduced graphene oxide/iron oxide nanocomposite catalyst for the oxygen reduction reaction, ChemistrySelect 1 (2016) 3640–3646.
[35] X. Wang, N.S.J. Gao, Q.X. Zhou, Concentration responses of toxicity sensor with *Shewanella oneidensis* MR-1 growing in bioelectrochemical systems, Biosens. Bioelectron. 43 (2013) 264–267.
[36] T. Li, X. Wang, L. Zhou, J.K. An, J.H. Li, N. Li, H.W. Sun, Q.X. Zhou, Bioelectrochemical sensor using living biofilm to in situ evaluate flocculant toxicity, ACS Sens. 1 (2016) 1374–1379.
[37] A.A. Carmona-Martinez, F. Harnisch, U. Kuhlicke, T.R. Neu, U. Schroder, Electron transfer and biofilm formation of *Shewanella putrefaciens* as function of anode potential, Bioelectrochemistry 93 (2013) 23–29.
[38] K. Rabaey, N. Boon, S.D. Siciliano, M. Verhaege, W. Verstraete, Biofuel cells select for microbial consortia that self-mediate electron transfer, Appl. Environ. Microb. 70 (2004) 5373–5382.
[39] C.I. Torres, A.K. Marcus, P. Parameswaran, B.E. Rittmann, Kinetic experiments for evaluating the Nernst-Monod model for anode-respiring bacteria (ARB) in a biofilm anode, Environ. Sci. Technol. 42 (2008) 6593–6597.
[40] Y.Y. Yu, C.X. Guo, Y.C. Yong, C.M. Li, H. Song, Nitrogen doped carbon nanoparticles enhanced extracellular electron transfer for high-performance microbial fuel cells anode, Chemosphere 140 (2015) 26–33.
[41] E. Marsili, D.B. Baron, I.D. Shikhare, D. Coursolle, J.A. Gralnick, D.R. Bond, *Shewanella* secretes flavins that mediate extracellular electron transfer, Proc. Natl. Acad. Sci. 105 (2008) 3968–3973.
[42] C.I. Torres, R. Krajmalnik-Brown, P. Parameswaran, A.K. Marcus, G. Wanger, Y.A. Gorby, B.E. Rittmann, Selecting anode-respiring bacteria based on anode potential: phylogenetic, electrochemical, and microscopic characterization, Environ. Sci. Technol. 43 (2009) 9519–9524.
[43] D. Sun, S.A. Cheng, A.J. Wang, F.J. Li, B.E. Logan, K.F. Cen, Temporal-spatial changes in viabilities and electrochemical properties of anode biofilms, Environ. Sci. Technol. 49 (2015) 5227–5235.
[44] X. Wei, L.C. Fang, P. Cai, Q.Y. Huang, H. Chen, W. Liang, X.M. Rong, Influence of extracellular polymeric substances (EPS) on Cd adsorption by bacteria, Environ. Pollut. 159 (2011) 1369–1374.
[45] J. Ha, A. Gélabert, A.M. Spormann, G.E. Brown, Role of extracellular polymeric substances in metal ion complexation on *Shewanella oneidensis*: batch uptake, thermodynamic modeling, ATR-FTIR, and EXAFS study, Geochim. Cosmochim. Acta 74 (2010) 1–15.
[46] Z.C. Wang, M.C. Gao, S. Wang, Y.J. Xin, D. Ma, Z.L. She, Z. Wang, Q.B. Chang, Y. Ren, Effect of hexavalent chromium on extracellular polymeric substances of granular sludge from an aerobic granular sequencing batch reactor, Chem. Eng. J. 251 (2014) 165–174.

[47] W. Liu, J.S. Zhang, Y.J. Jin, X. Zhao, Z.Q. Cai, Adsorption of Pb (II), Cd (II) and Zn (II) by extracellular polymeric substances extracted from aerobic granular sludge: efficiency of protein, J. Environ. Chem. Eng. 3 (2015) 1223–1232.
[48] A. Rahman, M. Mosquera, W. Thomas, J.A. Jimenez, C. Bott, B. Wett, A. Al-Omari, S. Murthy, R. Riffat, H. De Clippeleir, Impact of aerobic famine and feast condition on extracellular polymeric substance production in high-rate contact stabilization systems, Chem. Eng. J. 328 (2017) 74–86.
[49] B.E. Logan, Exoelectrogenic bacteria that power microbial fuel cells, Nat. Rev. Microbiol. 7 (2009) 375–381.
[50] A. Montebelli, R. Lowe, I. Ieropoulos, C. Melhuish, J. Greenman, T. Ziemke, Microbial fuel cell driven behavioral dynamics in robot simulations, Proceedings of the 12th International Conference on the Synthesis and Simulation of Living Systems 2010, pp. 749–756.
[51] D.L. Wang, P. Liang, Y. Jiang, P.P. Liu, B. Miao, W. Hao, X. Huang, Open external circuit for microbial fuel cell sensor to monitor the nitrate in aquatic environment, Biosens. Bioelectron. 111 (2018) 97–101.
[52] D. Tashima, K. Kurosawatsu, M. Uota, T. Karashima, M. Otsubo, C. Honda, Y. Sung, Space charge distributions of an electric double layer capacitor with carbon nanotubes electrode, Thin Solid Films 515 (2007) 4234–4239.
[53] M. Méndez-Tovar, J.V. García-Meza, I. González, Electrochemical monitoring of *Acidithiobacillus thiooxidans* biofilm formation on graphite surface with elemental sulfur, Bioelectrochemistry 128 (2019) 30–38.
[54] G.C. Gil, I.S. Chang, B.H. Kim, M. Kim, J.K. Jang, H.S. Park, H.J. Kim, Operational parameters affecting the performance of a mediator-less microbial fuel cell, Biosens. Bioelectron. 18 (2003) 327–334.
[55] Y. Jiang, P. Liang, P.P. Liu, Y.H. Bian, B. Miao, X.L. Sun, H.L. Zhang, X. Huang, Enhancing signal output and avoiding BOD/toxicity combined shock interference by operating a microbial fuel cell sensor with an optimized background concentration of organic matter, Int. J. Mol. Sci. 17 (2016) 1392.